Металлофиз. новейшие технол. / Metallofiz. Noveishie Tekhnol.
2014, т. 36, № 10, сс. 1399–1410
Оттиски доступны непосредственно от издателя
Фотокопирование разрешено только
в соответствии с лицензией

ДЕФЕКТЫ КРИСТАЛЛИЧЕСКОЙ РЕШЁТКИ

PACS numbers: 02.70.Ns, 61.72.Bb, 61.72.Mm, 61.72.sh, 61.72.Yx, 66.30.je, 82.60.Cx

Grain-Boundary Diffusion of Hydrogen Atoms in the α-Iron

S. M. Teus and V. G. Gavriljuk

G. V. Kurdyumov Institute for Metal Physics, N. A. S. of Ukraine,
36 Academician Vernadsky Blvd.,
UA-03680 Kyyiv-142, Ukraine

Grain boundary diffusion of hydrogen atoms in the α-iron is analysed based on the theoretical modelling. By means of molecular-dynamics simulation of hydrogen-atoms' migration in selected special grain boundaries with different misorientation angles as well as in the bulk, it is demonstrated that the activation enthalpy of hydrogen migration in the grain boundary is higher than that in the bulk. Based on this result, a conclusion is made that grain boundaries in the iron are traps for hydrogen atoms and retard their migration. As supposed, an increase in the hydrogen grain-boundary diffusion, as observed in some experiments, is related to the hydrogen-caused intergranular cracking.

За допомогою теоретичного моделювання було проаналізовано зерномежову дифузію атомів водню в α-залізі. Молекулярно-динамічне моделювання міґрації атомів водню в обраних межах зерен з різними кутами дезорієнтації, а також в об'ємі зерна, показало, що ентальпія активації міґрації атомів водню по межах зерен вища, ніж відповідне значення в об'ємі зерна. На підґрунті цих результатів зроблено висновок, що межі зерен у залізі є пастками для атомів водню і сповільнюють їх міґрацію. Зроблено припущення, що збільшення коефіцієнта зерномежової дифузії водню, яке спостерігалося в деяких експериментах, пов'язане з індукованим воднем міжкристалітним розтріскуванням.

Посредством теоретического моделирования исследована зернограничная диффузия атомов водорода в α-железе. Молекулярно-динамическое моделирование миграции атомов водорода в выбранных границах зёрен с разными углами разориентировки, а так же в объёме зерна, показало, что энтальпия активации миграции атомов водорода по границам зёрен выше, чем соответствующее значение в объёме зерна. Основываясь на этих результатах, сделан вывод, что границы зёрен в железе являются ловушками для атомов водорода и замедляют их миграцию. Сделано предположение, что увеличение коэффициента зернограничной диффузии водоро-

да, наблюдавшееся в некоторых экспериментах, связано с индуцированным водородом межкристаллитным растрескиванием.

Key words: α-iron, hydrogen-in-metal diffusion, special grain boundaries, molecular dynamics.

(Received 24 February, 2014)

1. INTRODUCTION

The phenomenon of materials degradation by hydrogen atoms, which is denoted as hydrogen embrittlement, takes important place in the modern material science. In practice, it appears as a substantial change in the mechanical behaviour of materials being exposed to severe hydrogen environment [1–3]. Under such conditions, the fracture takes place under applied stresses, which are much lower as compared to those for hydrogen-free materials [4]. The analysis of hydrogen interaction with different structural defects like dislocations, grain boundaries, and precipitates, is important to understand the peculiarities of hydrogen embrittlement. Taken into account that majority of materials used in industry are polycrystals and that the volume fraction of grain boundaries is usually high, the analysis of interaction between this structural defect and hydrogen atoms is of both scientific and practical significance (see, *e.g.*, [5–12]). After the penetration into material, the redistribution of hydrogen atoms can occur *via* different mechanisms, for example by the lattice or grain-boundary diffusion, as well as *via* dislocation transport. Among such diffusion pathways, a particular attention to the grain-boundary diffusion is related with the idea that the grain boundaries are the fastest diffusion paths. Nevertheless, the analysis of experimental data reveals that this approach is rather controversial. By measuring tritium concentration profile in 304 and 316 austenitic steels, Calder *et al.* [13] have shown that the grain-boundary diffusion coefficient was by eight orders of magnitude higher than that in the bulk. Using secondary ion mass spectrometry (SIMS), Tsuru and Latanision [14] analysed hydrogen permeation in the polycrystalline nickel. With the same techniques, Ladna and Birnbaum [15] studied the hydrogen depth distribution profile. Both of these studies have shown that grain boundaries increase the hydrogen diffusion in nickel. Nevertheless, in the first case, the diffusivity enhancement was about a factor within 60 to 100, whereas in the second one the enhancement was reported to be in the range of 8 to 17 times. Kimura and Birnbaum [16] also observed the acceleration of hydrogen migration along the grain boundaries in nickel. However, in this case, the reported level of diffusion enhancement was only of a factor two.

As it is seen from the mentioned experimental results, the data of

accelerated hydrogen grain-boundary diffusion are extremely different even in case of one material. It is also confusing that the increase of hydrogen grain-boundary diffusion in the austenitic steels is by several orders of magnitude higher than that in nickel, although the activation enthalpy for hydrogen migration in nickel is much lower in comparison with that in austenitic steels (0.4 eV for nickel [17] and in the range of 0.52 to 0.57 eV in CrNi austenitic steels [18]). While analysing the grain-boundary diffusion of hydrogen in nickel [15], it was reported that the enhancement exists only along the Σ3 and not along the Σ11 boundaries. This result was attributed to the difference in the energy of these boundaries. In other words, the increase of hydrogen diffusion along the grain boundaries cannot be considered as a general rule.

In contrast to the above-mentioned results, the enhancement of hydrogen diffusion along the grain boundaries was not confirmed in some studies (*e.g.*, [19, 20]), and moreover, the opposite results were obtained [21]. A comparison between the diffusion of hydrogen atoms in the single crystal and nanocrystalline palladium was performed in [22]. It was demonstrated that, at small hydrogen concentrations, the effective diffusion coefficient is higher in single crystal Pd, which suggests that the grain boundaries limit the hydrogen atoms mobility. With increasing hydrogen content, the effective diffusion in the nanocrystalline Pd starts to dominate.

The results mentioned above reveal that additional studies of hydrogen grain-boundary diffusion are necessary. In the present paper, the analysis is made based on the theoretical modelling. By means of theoretical calculations, it is possible to separate effects caused by hydrogen diffusion from other phenomena in materials, which can occur during experimental studies.

2. THEORETICAL CALCULATIONS

To study diffusion of hydrogen in the α-iron and the interaction of hydrogen atoms with the grain boundaries, a classical molecular-dynamics simulation was carried out using the large-scale atomic/molecular massively parallel simulator (LAMMPS) program package [23].

Taking into account a very low solubility of hydrogen in the α-iron, a single crystal of pure iron of bcc structure with dimensions of about 143×143×143 $Å^3$ was constructed with crystallographic orientations <100>, <010> and <001>. This single crystal contains approximately 250000 atoms. The symmetric-tilt grain boundaries were generated within the framework of the coincidence site lattice (CSL) theory [24, 25]. According to this theory, a symmetric tilt grain boundary is created by rotating the two parts of the single crystal around the tilt axis

and connecting them along the boundary. In general, the crystallography of grain boundary could be described by the five independent macroscopic parameters: the three to specify the mutual misorientation and the two to determine the grain-boundary plane. In our case, the rotation axis is <001> and the grain-boundary planes are (310), (410), and (710). An energy minimization procedure was applied to get an equilibrium configuration with the minimum energy value. The simulation cells for each case have a rectangular shape and the side lengths were chosen to satisfy the CSL conditions. For all the cells, periodic boundary conditions were applied.

The hydrogen atoms were homogeneously distributed over the whole volume of the cells, taking into account the well-known data that hydrogen atoms thermodynamically prefer to occupy the tetrahedral interstitial sites of the b.c.c. lattice [26, 27]. For all the simulations, the hydrogen concentration does not exceed 2 mass ppm, *i.e.*, the content that can be obtained experimentally, for the comparison.

To characterize atomic interactions, a potential developed in [28] from the embedded atom method potential [29–31] was considered. For the Fe–H interaction, an extensive database of energies and atomic configurations obtained by the density functional theory (DFT) calculations was used in order to fit the cross interaction between Fe and H.

Initially, all the systems were relaxed using Gibbs *NPT* ensemble. The pressure parameter (*P*) during the relaxation was controlled using the Parrinello–Rahman technique [32]. The Nose–Hoover method [33, 34] was used, to keep a constant temperature (*T*). The pressure was maintained at 0 Pa in all the simulations. Afterwards, we used Gibbs *NVT* thermodynamic ensemble to monitor the atomic positions during the steps of molecular dynamics. The *NPT* ensemble was applied for 500 ps to reach and stabilize the parameters at certain temperature and, thereafter, *NPT* ensemble was used for 100 ps to monitor the atomic positions at constant volume (*V*) and temperature.

To simulate a hydrogen permeation process, a supercell of b.c.c. iron with a dimensions $90\times180\times85$ Å^3 had been created with a high-angle special grain boundary $\Sigma5$ (310)[001]. The grain-boundary plane was created orthogonal to the surface along <100> crystal orientation. Initially, the hydrogen atoms were homogenously distributed on the crystal surface along <010> crystallographic axis, *i.e.*, orthogonal to the grain-boundary plane.

In the course of experimental measurements of hydrogen permeation, the electric potential is applied to create a hydrogen flux in a sample. To realize the same condition during simulation, an additional force was applied to all hydrogen atoms along <100> axis. The value of this force should satisfy two conditions: (i) it should provide the movement of hydrogen atoms along the force direction, instead of random walk; (ii) the energy created by this additional force component

should not significantly exceed the activation enthalpy of hydrogen migration, otherwise the difference between the hydrogen movement in the bulk and in the grain boundary will be hidden. The temperature of simulation was equal to 300 K.

3. RESULTS

Starting from the initial homogeneous distribution of hydrogen atoms over the simulation cell, the relaxation using *NPT* ensemble results in the change of spatial distribution of hydrogen. After the selected simulation time, the hydrogen atoms segregated to the grain boundaries. This atomic redistribution is shown in Fig. 1. The obtained result is consistent with the experimental data reported in [35, 36].

During the simulation, the mean square displacement parameter (MSD) was determined, which characterizes the spatial extent of random motion of hydrogen atoms. Afterwards, based on the MSD, the diffusion coefficient was derived following the Einstein expression:

$$D = \frac{1}{6t}\,\mathrm{MSD} = \frac{1}{6t}\left\langle \left| r(t) - r(0) \right|^2 \right\rangle, \qquad (1)$$

where t is a time interval, $r(t) - r(0)$ is a distance travelled by atom over a time interval t. The time variation of the mean square dependence parameter for hydrogen atoms in the bulk iron for different temperatures is shown in Fig. 2. The linear part on each curve allows determining the diffusion coefficient of hydrogen atoms at certain temperature. In the insert to Fig. 2, the dependence of hydrogen diffusion coefficient on the inverse temperature is shown.

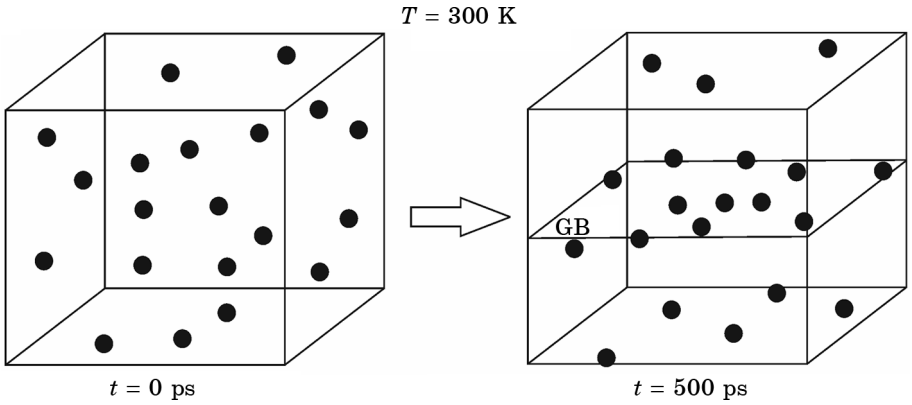

Fig. 1. Schematic view of hydrogen atoms redistribution when the grain boundary is present in comparison with the bulk as a result of molecular-dynamics simulation.

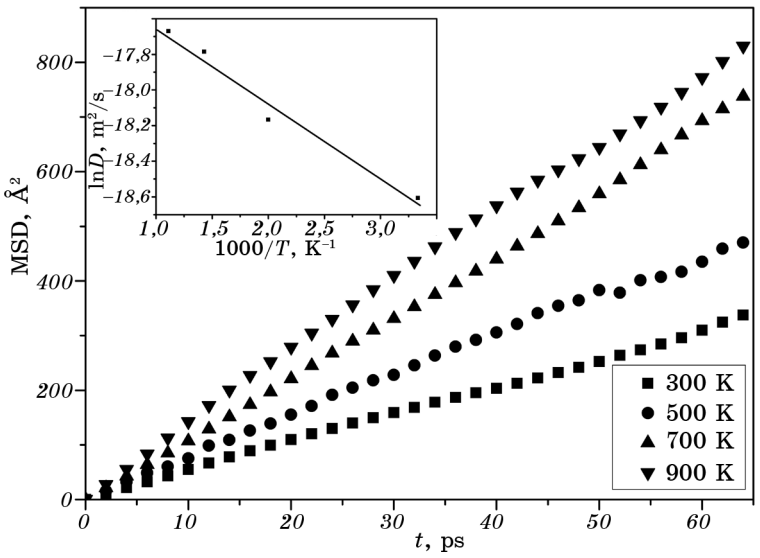

Fig. 2. Time dependence of mean square displacement for hydrogen atoms in the bulk α-iron at different temperatures. The insert shows the Arrhenius dependence of hydrogen diffusion coefficient versus reciprocal temperature.

A comparison could be made between the calculated hydrogen diffusion coefficient at room temperature and results of other theoretical calculations, as well as experimental data. In comparison with other molecular-dynamics data, our result ($D = 0.83 \cdot 10^{-8}$ m^2/s) is several times higher, but similar to the data obtained using the centroid path-integral molecular dynamics [37]. At the same time, our data are consistent with the experimental results [38, 39]. The discrepancy with other calculations could be related to the potential used in the present study, which describes the Fe–H and H–H interactions more correctly. It must be also mentioned about the scattering of the experimental data that strongly depends on the specimen purity.

In Figure 3, the temperature dependence of diffusion coefficient is shown for hydrogen atoms in the α-iron with different types of special grain boundaries. The analysis of such dependences in the Arrhenius co-ordinates allows determining the activation enthalpy for hydrogen atoms diffusion in the bulk and in the grain-boundary region. The calculated data are presented in Table.

As follows from Table, the dependence of the grain-boundary energy on the misorientation angle is in agreement with the trend that was previously reported by Shibuta *et al.* [40] and Jaatinen *et al.* [41]. Therefore, it is confirmed that there are some energy cusps in such dependence, which could be explained by a special atomic ordering, which causes a change in the grain-boundary energy.

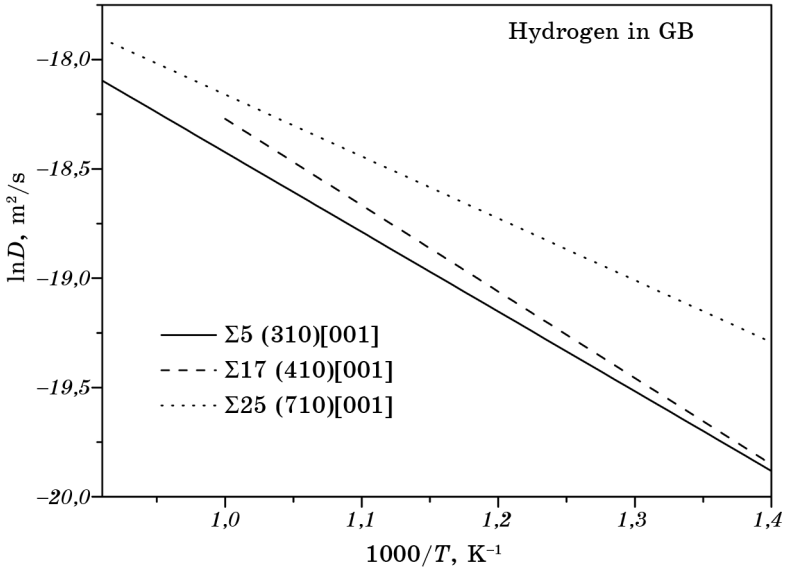

Fig. 3. Arrhenius dependence of hydrogen diffusion coefficient on reciprocal temperature for three cases of special grain boundaries.

A perfect agreement is obtained between the data calculated in the present study and the experimental activation enthalpy for the bulk hydrogen diffusion [39, 42]. The comparison of these data with those obtained for the system containing grain boundaries clearly shows that the activation enthalpy for diffusion of hydrogen in the vicinity of the grain boundary is always higher.

The result of simulation of hydrogen permeation process is presented in Fig. 4, where only the hydrogen atoms are shown and the graphical analysis of these data is represented in Fig. 5. Starting from the homogeneous distribution of hydrogen atoms on the one side of a crystal containing a grain boundary, the concentration profile is significantly modified with a time. As seen, the average penetration distance

TABLE. Characteristics of grain boundaries and results of molecular-dynamics study.

	Misorientation Angle, Θ°	Σ	Energy, mJ/m^2	Activation Enthalpy Hydrogen, eV
Bulk				0.037 ± 0.004
(310)[001]	36.87	5	1073	0.314 ± 0.017
(410)[001]	28.07	17	1102	0.341 ± 0.011
(710)[001]	16.26	25	1023	0.244 ± 0.001

of hydrogen atoms in the grain boundary is smaller than in the bulk that corresponds to different values of the hydrogen diffusion coefficient in these two areas.

4. DISCUSSION

The models used for the analysis of many experimental data about grain-boundary diffusion are based on the prediction that grain boundaries are the fast diffusion path (see, *e.g.*, [43–45]). However, it has to be mentioned that the theory used in such models was developed for the case of vacancy migration. The vacancy mechanism is traditionally used for the description of the enhanced grain-boundary diffusion of substitutional atoms. Therefore, taking into account that the grain boundaries are characterized by an increased concentration of vacancies, it seems to be natural that the grain-boundary diffusion of substitutional elements should be increased. This is consistent with all the experimental data where the grain-boundary diffusion of substitutional atoms is studied.

However, in case of the grain-boundary migration of interstitial atoms, vacancies cannot accelerate the diffusion of hydrogen atoms. Moreover, the hydrogen atoms form complexes with vacancies in the α-iron. It reduces their mobility as the binding energy in the hydrogen-vacancy complexes is added to the migration enthalpy energy. A strong

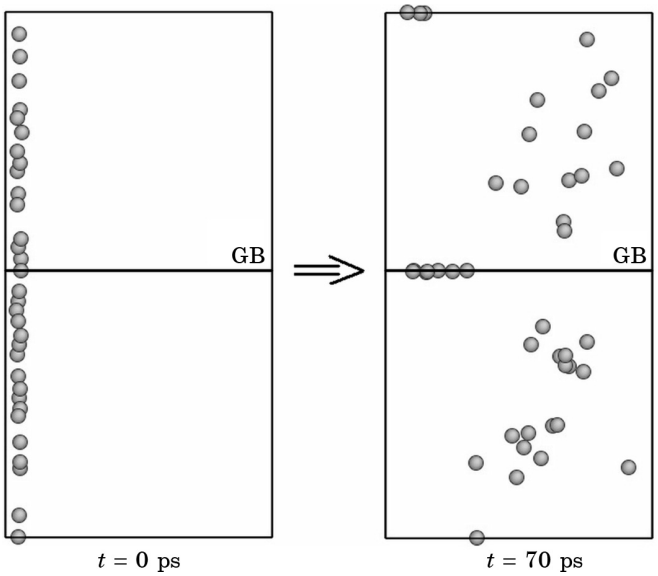

Fig. 4. Schematic representation of hydrogen atoms redistribution in the α-iron sample with Σ5 (310) special grain boundary after the time interval t.

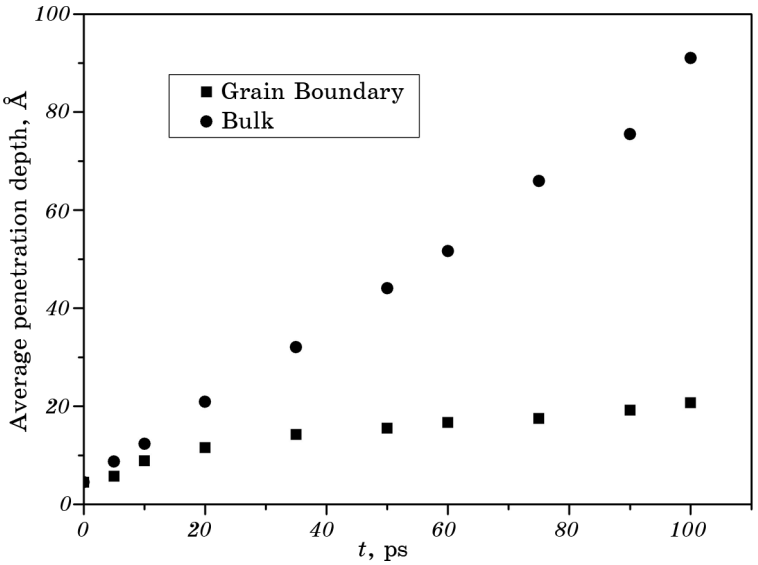

Fig. 5. Molecular-dynamics simulation of hydrogen penetration in the α-iron crystal with Σ5 (310) special grain boundary. Initially, the hydrogen atoms were homogeneously distributed on the surface of the simulated crystal. The crystal size is of 90×180×85 Å^3.

affinity of hydrogen atoms to vacancies in the iron follows from the *ab-initio* calculations [46].

The segregation factor is an important parameter that is included in many theoretical equations used for the analysis of experimental data obtained using the autoradiography, sectioning method or SIMS. Taking into account difficulties of a direct determination of this parameter, on the one hand, and a strong affinity of hydrogen atoms with the grain boundaries, on the other hand, (see Refs. [35, 36]), the analysis of experimental data is quite complicated, which could be a reason for such a big scatter in the experimental results, as mentioned in the Introduction. In this relation, the theoretical modelling has an advantage because the mobility of atoms directly located in the area of grain boundary should be taken into consideration. An advantage of theoretical modelling was also demonstrated in [47], where the theoretical predictions were formulated for observation of the enhanced grain-boundary diffusion of hydrogen. Nevertheless, its application to experimental measurements of hydrogen penetration in nickel [48] has shown that the grain boundaries are not high diffusion path for hydrogen.

Our molecular-dynamics simulations show that grain boundaries retard migration of hydrogen atoms. As follows from the comparison between the values of activation enthalpy for diffusion of hydrogen in

the bulk and in the vicinity of the grain boundary (see Table), the latter is higher for all studied types of grain boundaries. It means that diffusion along the grain boundaries should be decreased. This result suggests that grain boundaries act as traps for hydrogen atoms and cannot be a high diffusion path for them.

A simple physical substantiation can be proposed for the retarded migration of hydrogen atoms along the grain boundaries. If hydrogen atoms in the solid solution approach the grain boundary (the tendency of hydrogen atoms to grain-boundary segregation also follows from our modelling), the elastic term disappears from the chemical potential gradient or significantly decreases. Thus, the grain-boundary migration of such atoms cannot be faster in comparison with that in the bulk. An additional argument is that interstitial atoms create complexes with the vacancies in the grain-boundary region, which also reduces their mobility. It should be noted that we do not consider the case when the density of grain boundaries is increased significantly that could be in case of severe plastic deformation with the formation of nonequilibrium grain boundaries [49].

To explain the experimentally observed acceleration of hydrogen diffusion along the grain boundaries (*e.g.*, in [13, 17, 50]), which is in contradiction with the results of our theoretical modelling, the following approach could be proposed. During electrolytic charging, hydrogen atoms enter the bulk of the material and are redistributed there, according to their affinity with the crystal-lattice defects. In the aged material, the grain boundaries are the main lattice defects. Therefore, based on the hydrogen enhanced localized plasticity mechanism (HELP) in its elasticity [51] or electron interpretations [52], the formation of hydrogen atmospheres in the vicinity of the grain boundaries should result in some reduction of the stress needed for opening of microcracks. Thus, an increased migration of hydrogen atoms, as observed in some experiments, can be a consequence of the hydrogen-induced grain-boundary microcracking with the further molecular hydrogen recombination in these cracks, its repeated dissociation at the crack tips, and migration along the grain boundary.

The detailed analysis of experimental results presented in [50] shows also that, at the initial stage of the hydrogen permeation process, the flux is larger in the coarse grain specimens. With increasing time, the hydrogen flux in the small grain material became larger. This result can be evidence that, at the beginning, the grain boundaries act as traps for hydrogen atoms and, only after the crack formation, the hydrogen migration is intensified in the samples with smaller grains.

The suggested microcracking along the grain boundaries in the course of hydrogen charging of the samples is also applied to the results presented in [22], where, at high hydrogen contents, the hydrogen grain-boundary diffusion coefficient is higher than that in the

bulk. According to our approach, the increase in the density of hydrogen clouds around the grain boundaries results in the microcracks' initiation caused by the operating HELP mechanism or the brittle phase formation along the grain boundaries. Both effects can lead to the increase in the effective hydrogen diffusion coefficient in the nanocrystalline Pd.

5. CONCLUSIONS

The role of the grain boundaries in the diffusion of hydrogen atoms in the α-iron was studied based on the molecular-dynamics simulations. It was shown that the migration activation enthalpy of hydrogen atoms located in the vicinity of high-angle grain boundaries is higher as compared to that in the bulk. The retardation of grain-boundary migration of hydrogen atoms is explained by the disappearance or the drastic decrease of the elastic term in the gradient of chemical potential due to capture of interstitial hydrogen atoms by the grain boundaries. An increase in grain-boundary diffusion coefficient, as observed in some experiments, can be related to the hydrogen-caused intergranular cracking, which accompanies the hydrogen penetration because of hydrogen segregation at the grain boundaries and corresponding hydrogen embrittlement.

REFERENCES

1. C. D. Beachem, *Metall. Trans. A*, **3**: 437 (1972).
2. I. M. Bernstain and A. W. Thompson, *Int. Met. Rev.*, **21**: 269 (1979).
3. J. P. Hirth, *Metall. Trans. A*, **11**: 861 (1980).
4. D. Symons, *Metall. Trans. A*, **29**: 1265 (1998).
5. H. Vehoff, *Hydrogen in Metals III* (Ed. H. Wipf) (Berlin–Heidelberg: Springer: 1997).
6. A. Pundt and R. Kirchheim, *J. Mater. Res.*, **36**: 555 (2006).
7. K. H. Lo, C. H. Shek, and J. K. L. Lai, *Mater. Sci. and Eng. R*, **65**: 39 (2009).
8. H. Fukushima and H. K. Birnbaum, *Acta Metal.*, **32**: 851 (1984).
9. P. Novak, R. Yuan, B. P. Somerday, P. Sofronis, and R. O. Ritchie, *J. Mech. Phys. Solids*, **58**: 206 (2010).
10. L. Zhong, R. Wu, A. J. Freeman, and G. B. Olson, *Phys. Rev. B*, **62**: 13938 (2000).
11. M. Wen, S. Fukuyama, and K. Yokogava, *Acta Mater.*, **51**: 1767 (2003).
12. Y. A. Du, L. Ismer, J. Rogal, T. Hickel, J. Neugebauer, and R. Drautz, *Phys. Rev. B*, **84**: 144121 (2011).
13. R. D. Calder, T. S. Elleman, and K. Verghese, *J. of Nuclear Mater.*, **46**: 46 (1973).
14. T. Tsuru and R. M. Latanision, *Scripta Metal.*, **16**: 575 (1982).
15. B. Ladna and H. K. Birnbaum, *Acta Metall.*, **35**: 2537 (1987).
16. A. Kimura and H. K. Birnbaum, *Acta Metall.*, **36**: 757 (1988).

17. A. M. Brass, A. Chanfreau, and J. Chene, *Hydrogen Effects on Material Behaviour* (Eds. A. W. Thompson and N. R. Moody) (Warrendale, Pennsylvania: TMS Publ.: 1990), p. 19.
18. N. R. Quick and H. H. Johnson, *Metall. Trans. A*, **10**: 67 (1979).
19. W. Beck, J. Bockris, J. McBreen, and L. Nanis, *Proc. R. Soc. A*, **290**: 220 (1966).
20. W. M. Robertson, *Z. Metallk.*, **69**: 436 (1973).
21. V. M. Sidorenko and I. I. Sidorak, *Physicochemical Mechanics of Materials*, **9**: 12 (1973).
22. R. Kirchheim, *Phys. Scr.*, Iss. T94: 58 (2001).
23. S. Plimpton, *J. Comp. Phys.*, **117**: 1 (1995).
24. S. Ranganathan, *Acta Cryst.*, **21**: 197 (1966).
25. M. A. Fortes, *phys. status solidi (b)*, **54**: 311 (1972).
26. D. E. Jiang and E. A. Carter, *Phys. Rev. B*, **70**: 064102 (2004).
27. J. K. Norskov, *Phys. Rev. B*, **26**: 2875 (1982).
28. A. Ramasubramaniam, M. Itakura, and E. Carter, *Phys. Rev. B*, **79**: 174101 (2009).
29. M. I. Mendelev, S. Han, D. J. Srolovitz, G. J. Ackland, D. Y. Sun, and M. Asta, *Philos. Mag.*, **83**: 3977 (2003).
30. G. J. Ackland, M. I. Mendelev, D. J. Srolovitz, S. Han, and A. V. Barashev, *J. Phys. Condens. Matter*, **16**: S2629 (2004).
31. M. W. Finnis and J. E. Sinclair, *Philos. Mag. A*, **50**: 45 (1984).
32. M. Parrinello and A. Rahman, *J. Appl. Phys.*, **52**: 7182 (1981).
33. S. Nose, *Mol. Phys.*, **52**: 255 (1984).
34. W. G. Hoover, *Phys. Rev. A*, **31**: 1695 (1985).
35. J. S. Wang, *Eng. Fract. Mech.*, **68**: 647 (2001).
36. T. Ohmisawa, S. Uchiyama, and N. Nagumo, *J. Alloys Compd.*, **356–357**: 290 (2003).
37. H. Kimizuka, H. Mori, and S. Ogata, *Phys. Rev. B*, **83**: 094110 (2011).
38. J. L. Dillard and S. Talbot-Besnard, *L'hydrogene Dans les Metaux* (Paris: Editions Science et Industrie: 1972), vol. **1**.
39. M. Nagano, Y. Hayashi, N. Ohtani, M. Isshiki, and K. Igaki, *Scr. Metall.*, **16**: 973 (1982).
40. Y. Shibuta, S. Takamoto, and T. Suzuki, *ISIJ International*, **48**: 1582 (2008).
41. A. Jaatinen, C. V. Achim, K. R. Elder, and T. Ala-Nissila, *Technische Mechanik*, **30**: 169 (2010).
42. J. F. Dufresne, A. Seeger, P. Groh, and P. Moser, *phys. status solidi (a)*, **36**: 579 (1976).
43. T. Suzuoka, *Trans. Japan Inst. Metals*, **2**: 25 (1961).
44. J. C. Fisher, *J. Appl. Phys.*, **22**: 74 (1951).
45. R. T. P. Whipple, *Philos. Mag.*, **45**: 1225 (1954).
46. R. Nazarov, T. Hickel, and J. Neugebauer, *Phys. Rev. B*, **82**: 224104 (2010).
47. J. Yao and J. R. Cahoon, *Acta Metal Mater.*, **39**: 111 (1991).
48. J. Yao and J. R. Cahoon, *Acta Metal Mater.*, **39**: 119 (1991).
49. A. A. Nazarov, A. E. Romanov, and R. Z. Valiev, *Acta Metall. Mater.*, **41**: 1033 (1993).
50. A. M. Brass and A. Chanfreau, *Acta Mater.*, **44**: 3823 (1996).
51. H. K. Birnbaum and P. Sofronis, *Mat. Sci. Eng. A*, **176**: 191 (1994).
52. V. G. Gavriljuk, B. D. Shanina, V. N. Shyvanyuk, and S. M. Teus, *J. Appl. Phys.*, **108**: 083723-1–9 (2010).